Morphological Studies of Binary Mixtures of Block Copolymers: Temperature Dependence of Cosurfactant Effects

François Court,[†,‡,§] Daisuke Yamaguchi,[†,⊥] and Takeji Hashimoto*,[†,⊥]

Department of Polymer Chemistry, Graduate School of Engineering, Kyoto University, Katsura, Nishikyo-ku, Kyoto 615-8510, Japan, and Laboratoire de Physico-Chimie Structurale et Macromoléculaire, ESPCI, 10 rue Vauquelin, 75005 Paris, France

Received November 25, 2005; Revised Manuscript Received January 24, 2006

ABSTRACT: A unique phase behavior was investigated for binary mixtures of diblock copolymers in order to explore the cosurfactant effect as a function of temperature. The mixtures are composed of a long asymmetric polystyrene-*block*-polyisoprene (SI) copolymer and a short symmetric SI copolymer denoted, respectively, as *as* and s_3. The neat *as* copolymer forms polystyrene (PS) spherical microdomains on a body-centered-cubic lattice in polyisoprene (PI) matrix from ambient temperature to 180 °C, while neat s_3 is always in the disordered state in the same temperature range. The mixtures of $as/s_3 = 45/55$ and 75/25 (w/w) are mainly focused in this study. Both of them show lamellar morphology at low temperatures, then undergo an "order−order transition (OOT)" to a "bicontinuous structure" with a considerable distortion in the long-range order, and finally reach the truly disordered state through the "order−disorder transition (ODT)" with increasing temperature. The reason why quotation marks were put in "OOT" and "ODT" is explained in the text. We found that the invariants (the integrated scattered intensity) do not change across the "OOT" for these two mixtures. It is intriguing to note that these two mixtures exhibit a quite opposite temperature dependence of the characteristic length *D* for the ordered structures, which seems to be related to the "cosurfactant effect" as discussed in the text. The cosurfactant effect was shown to decrease with increasing temperature and to promote the distorted bicontinuous phase.

I. Introduction

In this series of work, we explore morphological behavior of a series of binary mixtures of polystyrene (PS)-*block*-polyisoprene (PI) diblock copolymer (SI) composed of a long asymmetric SI denoted as *as* having degree of polymerization (DP) denoted as N_{as} and a short symmetric SI denoted as s_i ($i = 1$, 2, or 3) having varying DP's denoted as N_{si} ($i = 1$, 2, or 3). In the previous works the mixtures were examined at ambient temperature, and the following features were elucidated.[1] All the mixtures studied were miscible at molecular level, yielding a single ordered morphology or a disordered single phase. A phase diagram previously investigated in the parameter space of the ratio of DP, $r \equiv N_{as}/N_{si}$, and overall volume fraction of PS block in the mixture ϕ_{PS} is summarized in Figure 1. Although the morphologies encountered are the common ones found in pure SI copolymers, such as spheres in body-centered-cubic lattice (Sph), hexagonal cylinders (Cyl), bicontinuous structures (Bic), and lamellae (Lam), the stability limit of each morphology for the mixture is significantly shifted with respect to ϕ_{PS} from that for corresponding neat block copolymer. More interestingly, the shift of the morphological boundary increases with increasing the ratio *r*. As a consequence, mixing of a small amount of the symmetric blocks s_i ($i = 1$, 2, or 3) into the majority component of asymmetric blocks *as* effectively decreases the interface curvature and hence enlarges the composition range where the lamellar microdomains are developed. This so-called **cosurfactant effect**, i.e., the effects that two block copolymers having different block lengths display when they share a common interface, was found to become more remarkable as *r* (or the molecular weight ratio) gets bigger.

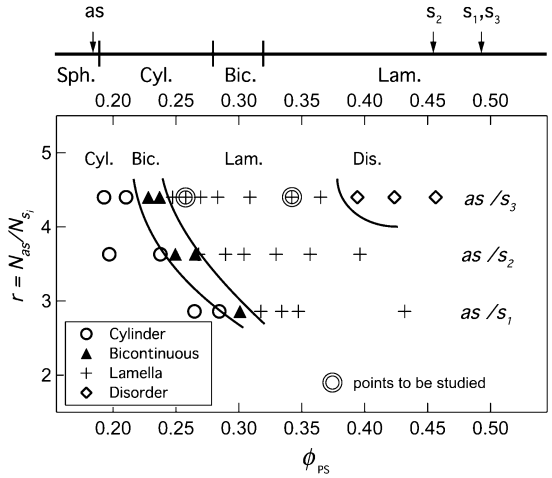

Figure 1. Phase diagram of as/s_i ($i = 1$, 2, and 3) mixtures investigated at ambient temperature, which was obtained by part 1 of this series of papers.[1] Morphology variation is shown in the parameter space of *r* and ϕ_{PS}. $as/s_3 = 45/55$ and 75/25 mixtures, marked by double circle, are investigated along the temperature axis in this study.

In this paper we focus our attention on how the cosurfactant effect or the boundary between different morphology shown in Figure 1 changes with temperature and how the mixture reaches disordered state with raising temperature. Our study of the temperature effect was focused on the as/s_3 mixtures, in which the difference in the molecular weights of the constituent copolymers is the largest, giving rise to the most remarkable cosurfactant effects, and the disordered state is most easily attained due to the lowest molecular weight of s_3. The two blend samples marked by double circles with + mark inside in Figure

† Kyoto University.
‡ ESPCI.
§ Present address: Thiochemicals-ARKEMA S. A., 4-8 cours Michelet-La Défense 10, F 92091, Paris la Défense Cedex, France.
⊥ Present address: Advanced Science Research Center, Japan Atomic Energy Agency, Tokai-mura, Ibaraki Pref., 319-1195, Japan.
* To whom correspondence should be addressed. E-mail: hashimoto.takeji@jaea.go.jp.

10.1021/ma0525233 CCC: $33.50
Published on Web 03/03/2006

Table 1. Characteristics of the SI Diblocks

code	$\bar{M}_n \times 10^{-3}$ [a]	HI[b]	$\bar{M}_{nPS} - \bar{M}_{nPI} \times 10^{-3}$ [c]	$N_{PS} - N_{PI}$[d]	N[e]	w_{PS}[f]	f_{PS}[g]
as	47.0	1.03	9.6−37.4	92−550	642	0.205	0.185
s_3	12.1	1.03	6.3−5.8	61−85	146	0.52	0.49

[a] $\bar{M}_n$: number-average molecular weight determined by size exclusion chromatography (SEC). [b] HI $= \bar{M}_w/\bar{M}_n$: heterogeneity index for molecular weight distribution. [c] $\bar{M}_{nk}$: number-average molecular weight of the *k*th block (k = PS or PI). [d] N_k: number-average degree of polymerization of the k-th block (k = PS or PI). [e] N: total number-average degree of polymerization of the diblock: $N = N_{PS} + N_{PI}$. [f] w_{PS}: polystyrene weight fraction. [g] f_{PS}: volume fraction of the PS block calculated from $f_{PS} = (w_{PS}/\rho_{PS})/(w_{PS}/\rho_{PS}+(1 - w_{PS})/\rho_{PI})$ by using the following densities for the PS and PI blocks, $\rho_{PS} = 1.0514$ g cm^{-3} and $\rho_{PI} = 0.925$ g cm^{-3}.

1; i.e., *as*/s_3 = 45/55 and 75/25 (w/w) are particularly highlighted in this study. These mixtures present lamellar morphology at ambient temperature and are transformed into a "distorted bicontinuous morphology" with increasing temperature. Here the "distorted bicontinuous morphology" is meant to indicate the bicontinuous morphology having a sufficient distortion in its long-range order. Nevertheless, we define here this morphology as the one in an "ordered phase", simply because (i) the morphology shows a broad second-order peak or shoulder in SAXS (small-angle X-ray scattering) profiles and (ii) the morphology observed under transmission electron microscopy (TEM) on the specimens rapidly vitrified from the bicontinuous phase shows an unidentified bicontinuous morphology which is definitely different from the so-called fluctuation-induced disordered structure (D_F),[2,3] as detailed later in sections IV.1 and IV.2.

Thus, in this work a transition from the lamellar phase to the distorted bicontinuous phase is defined to be an "OOT (order−order transition)". As temperature is further raised above the "OOT" temperature (T_{OOT}), the second-order peak or shoulder in SAXS profiles disappears, and we define this temperature as the "ODT (order−disorder transition)" temperature (T_{ODT}). In the context of the current theory of "ODT", one defines the distorted bicontinuous phase as a part of disordered phase, and then our "OOT" in this work corresponds to "ODT". If one takes this context, one should read our "OOT" as "ODT", and one may note two kinds of the disordered states: (i) the state having distorted bicontinuous morphology and (ii) the disordered state which exhibits the thermal concentration fluctuations as described by the random phase approximation (RPA).[4] We aimed to elucidate the cosurfactant effects as a function of temperature and temperature-induced **"OOT" and "ODT" in the context of our definition**.

We are aware of a considerable number of studies focusing on the phase behavior of binary mixtures of diblock copolymers.[5−8] However, only a few of them pay attention to cosurfactant effects. Zhao et al.[9] examined the temperature dependence of morphology in the binary mixtures of poly(ethylene)-*block*-poly(ethylethylene) diblock copolymers. However, in their study the compositions of the two block copolymers and/or the molecular weights of the constituent copolymers were relatively similar so that the cosurfactant effect was hardly observed. From the viewpoint of controlling morphology by the mixing of two copolymers, the cosurfactant effect is an interesting and nontrivial problem, and its temperature effect is also important, as will be presented in this study.

II. Experimental Methods

II.1. Sample Preparation. SI diblock copolymers were prepared by sequential living anionic polymerization, as detailed in the previous publication.[1] Table 1 summarizes the characteristics of the synthesized diblocks, *as* and s_3. The film specimens of their binary mixtures, i.e., *as*/s_3 = 45/55 and 75/25 (w/w), were prepared in the following way. Solutions having 10 wt % of polymers in total were obtained by dissolving the two block copolymers with toluene as a neutrally good solvent for both PS and PI. The solutions in which the two block copolymers were mixed homogeneously in the disordered state were stirred for 5 h and then placed in a Petri dish in a temperature-controlled atmosphere at 25 °C. The slow evaporation process of the solvent lasted over 3 weeks. The film specimens were further dried at 80 °C under vacuum until constant weights were attained. The film specimens obtained by the casting process as described above were then employed for the in-situ temperature-dependent small-angle X-ray scattering (SAXS) measurements. Before SAXS measurements the film specimens were cut and stacked up the parallelepiped shape of 3 × 3 × 12 mm and packed into the sample holder and then preannealed at 180 °C for several hours to annihilate bubbles which were developed in the specimens upon annealing above glass transition temperature of PS phase ($T_{g,PS}$). During annealing and SAXS measurements the specimens were always placed under vacuum to suppress thermal degradation.

II.2. Small-Angle X-ray Scattering. The microdomain structures as a function of temperature were investigated by SAXS using a rotating anode X-ray generator operated at 50 kV and 200 mA.[10−12] The X-ray is monochromated so that its wavelength corresponds to the Cu Kα line (λ = 0.154 nm). The scattered intensity is measured with a one-dimensional position sensitive proportional counter with the sample-to-camera distance of 1166 mm. The SAXS profiles were corrected for air scattering, background scattering arising from thermal diffuse scattering (TDS) for most of the cases, unless otherwise stated, absorption, and slit-height and slit-width smearing effects.[10−15] The absolute SAXS intensity was determined by the nickel foil method.[16] The profiles are represented as a function of magnitude of scattering vector, q, which is related to the scattering angle, θ

$$q = (4\pi/\lambda)\sin(\theta/2) \quad (1)$$

The thermal protocol employed in the SAXS experiments is as follows. After annihilation of the bubbles, the preannealed specimen was further annealed for 2 h at 180 °C and then settled down to the highest temperature for the measurement. The first series of measurements at each temperature was conducted during the cooling process starting from the highest temperature, which was followed by the second series of measurements on the heating process from a low temperature to a high temperature. These two series of measurements permitted to confirm whether the specimen was in the equilibrium state at each temperature. A temperature change from one to another was finished within 15 min, and then the specimen was further held for 45 min at the set temperature before the SAXS measurement to attain its thermal equilibrium. The SAXS measurement lasted for 1 h at each set temperature.

II.3. Transmission Electron Microscopy. The microdomain structures were examined under transmission electron microscopy (TEM). Ultrathin sections of 40−50 nm in thickness were obtained from the film specimens using a Reichert ultramicrotome operated at −100 °C. The sections were then exposed to OsO_4 vapor for 1 h. This procedure is known to induce the selective staining and cross-linking of the double bonds of the polyisoprene with OsO_4.[17] The stained sections were observed with a Hitachi H-600S TEM operated at 100 keV. On the TEM pictures the PI microdomains appear dark, while the PS microdomains appear bright. The specimens employed for the TEM observation were the same ones employed for the SAXS measurement; therefore, the annealing

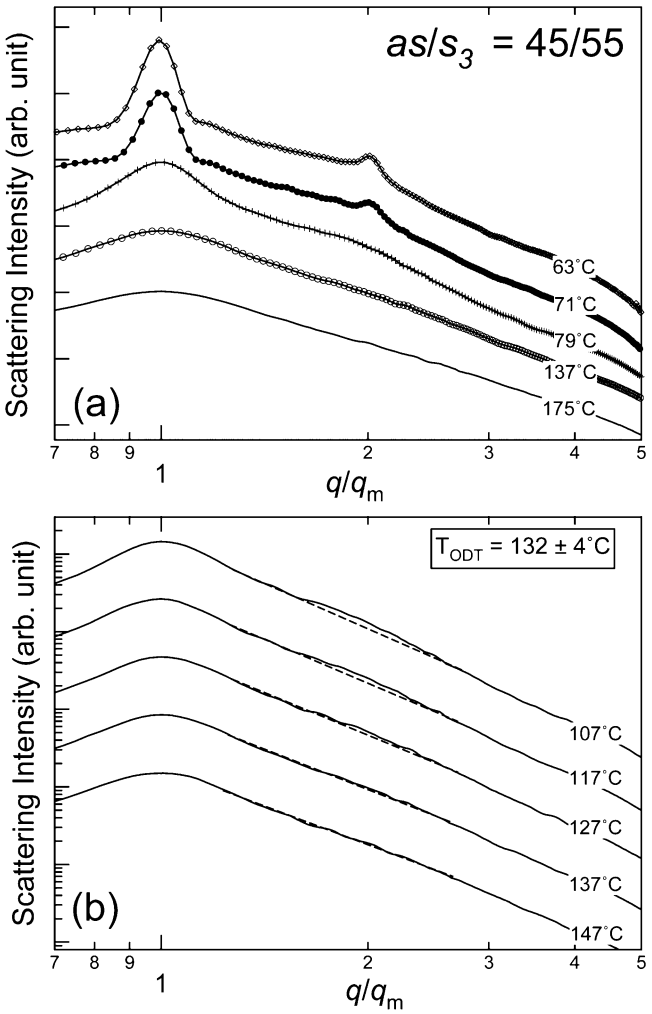

Figure 2. Small-angle X-ray scattering (SAXS) profiles of the $as/s_3 = 45/55$ mixture measured at different temperatures: (a) from 63 to 175 °C, the mixture undergoes "OOT" (between 71 and 79 °C) as well as "ODT" (between 79 and 137 °C); (b) in the vicinity of the "ODT" where the broken lines underneath of the measured scattering profiles (solid lines) are visual guides for the presence of the second-order broad peak or shoulder on the profiles. In both (a) and (b), the scattering curves are vertically shifted from each other by a factor of 5 in order to avoid overlap. The abscissa is not q itself but q normalized with q_m, q at scattering maximum.

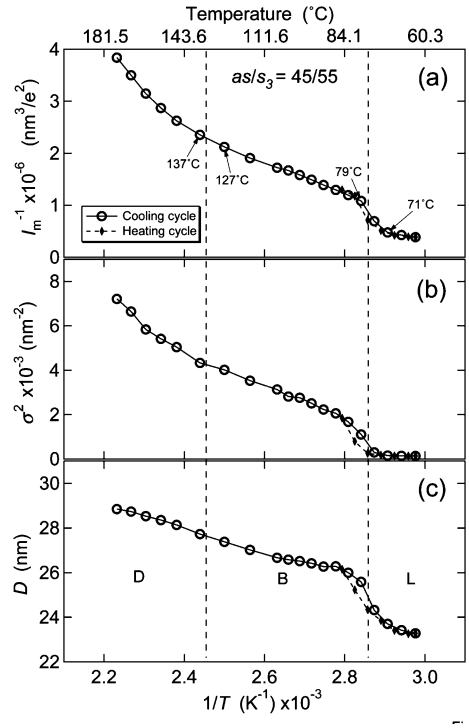

Figure 3. Plots for the $as/s_3 = 45/55$ mixture: influence of the temperature on inverse of the maximum of the first-order peak, I_m^{-1} (a), on square of the half-width at half-maximum of the first-order peak, σ_q^2 (b), and on the characteristic length of the microdomains or concentration fluctuations, D (c). The broken vertical lines separate the temperature ranges where the lamellae phase (L), the distorted bicontinuous phase (B), and the disordered phase (D) exist. The solid and broken lines were obtained in the cooling process and heating process, respectively.

process of the TEM specimen before quench is identical with that of SAXS measurement. A freezing of the microdomain structures, which are stable at high temperatures, was conducted by quenching the specimen into ice water. The success of the quench was confirmed by the comparison of the SAXS profiles taken before and after quench.

III. Results

III.1. $as/s_3 = 45/55$ Mixture. The scattering profile of the mixture $as/s_3 = 45/55$ measured at different temperatures is shown in Figure 2a,b. Note that in these figures the abscissa is not the magnitude of scattering vector q itself but normalized by q_m, which corresponds to the q value of the first-order scattering peak. Note that the variation of q_m with T can be seen by the variation of the spacing D with T in Figure 3 later as $q_m = 2\pi/D$. At a high temperature (175 °C), the scattering intensity profile shows only one broad peak with small intensity (Figure 2a), suggesting that the mixture is in the single phase where both *as* and s_3 are molecularly mixed in the disordered state. Above 137 °C the profiles conserve the same behavior. Contrarily, below 127 °C (Figure 2b) a shoulder or a broad peak was observed as well as the first-order peak. This shoulder peak located approximately at $q/q_m = 2$. When the temperature was decreased, the shoulder became distinct, while its relative position q/q_m looked unaltered. The presence of a shoulder suggests an ordered phase and that the spatial distribution of the electron density is not sinusoidal. The transition between disordered and ordered states, "ODT", is characterized in this manner, and the transition temperature, T_{ODT}, is estimated to be 132 ± 4 °C. The shoulder is relatively well identified at 79 °C and whose position is at $q/q_m = 1.9$. However, the space symmetry of the microdomain structure cannot be identified from that scattering profile alone. Contrarily, at 71 °C and below the scattering profile has a sharp and intensified first-order scattering peak and, moreover, a well-identified second-order scattering peak at the position of $q/q_m = 2$. Such a profile is characteristic of lamellar microdomain structure. The above results conclude (i) the $as/s_3 = 45/55$ mixture is in the disordered state at the temperatures ranging from 137 to 175 °C, (ii) it has the ordered lamellar microdomains at the temperatures below 71 °C, (iii) in the temperature range from 79 to 127 °C the mixture is in the ordered state other than the lamellar microdomains, and (iv) these changes with temperatures are thermoreversible.

I_m^{-1}, σ_q^2, and D, which are respectively the inverse peak scattered intensity, the square of the half-width at half-maximum of the peak, and the characteric length of the system, are shown respectively as a function of inverse of the temperature in parts a, b, and c of Figure 3. The change of the scattering profile between 79 and 71 °C is well reflected on the temperature dependence of these characteristic parameters. Actually, the three curves of I_m^{-1}, σ_q^2, and D present a discontinuity between

79 and 71 °C. These discontinuities are a signature of a phase transition between an ordered phase other than lamella and the lamellar phase, which is hereafter designated as order−order transition, "OOT". The former phase and the latter phase are stable at temperatures higher than 79 °C and lower than 71 °C, respectively. Since this temperature range is near the $T_{g,PS}$, a 1 h interval (or preannealing) between the successive measurements probably is expected to be too short compared to the time required for the completion of the structural change. Nevertheless, the results demonstrate that this "OOT" is thermally reversible approximately in the time scale of our observation. Contrarily, "ODT" cannot be identified by the discontinuities on the characteristic parameters of the first-order peak. The curves of I_m^{-1} and σ_q^2 vs T^{-1} in Figure 3a,b exhibited only the change in slope at "ODT", while the curve D vs T^{-1} did not even exhibit the change in the slope at "ODT". This behavior of $I_m^{-1}$and σ_q^2 at "ODT" is specific for the *as*/s_3 mixture and clearly different from those of pure diblock copolymer. In the case of pure block copolymer, $I_m^{-1}$and σ_q^2 present a very sharp discontinuity at T_{ODT}.[18−20]

The variation of D as a function of temperature is quite anomalous. In fact, in the temperature range investigated D increases with temperature. Since the mixture has a lamellar morphology below "OOT", this corresponds to an increase of lamella thickness with temperature. This result is physically anomalous, from the viewpoint that in the case of a pure SI copolymer D decreases with temperature. Actually, when T increases, the interaction parameter χ, which represents the net repulsive force between the PS and PI blocks, decreases. The chains are thus less stretched, and the thickness of lamellas decreases.[18,21] The anomalous behavior of D for the *as*/s_3 = 45/55 mixture will be discussed later in the Discussion section.

III.2. *as*/s_3 = 75/25 Mixture. The behavior of the scattering intensity profile of this mixture as a function of temperature is very similar to that of the *as*/s_3 = 45/55 mixture. Three different regimes are observed from the scattering intensity profiles plotted as a function of normalized scattering vector q/q_m in Figure 4a,b. The profiles measured at 70 and 95 °C exhibit a lamellar microdomain structure. Between 95 and 102 °C the first-order peak becomes broader and the second-order peak observed at $q/q_m \cong 1.9$ becomes even broader or a shoulder, suggesting a bicontinuous morphology as will be clarified later by TEM in section 4.1. It should be noted that the peak breadth for the bicontinuous phase is much smaller for this mixture than that for the 45/55 mixture. This fact becomes clearer when one compares Figures 3b and 5b, the latter being shown later. The disappearance of the shoulder between 166 and 173 °C (Figure 4b) may be identified as the "ODT". In fact, above this temperature the scattering profile of the *as*/s_3 = 75/25 mixture is characteristic of the disordered state as well described by RPA.

The behaviors of I_m^{-1}, σ_q^2, and D as a function of the inverse temperature are shown respectively in Figure 5a−c. Two transitions implied by the careful observation of change in the scattering profile with T are discerned in these plots also. "OOT" can be discerned by a discontinuity on the curves of I_m^{-1}, σ_q^2, and D vs T^{-1} (Figure 5a−c). On the other hand, "ODT" cannot be easily identified by Figure 5a−c. The curves of I_m^{-1}, σ_q^2, and D present neither discontinuity nor a change in the slope at T_{ODT}. It is determined only from the scattering profile itself, namely from existence or no existence of the shoulder peak located approximately at $q/q_m = 2$. These two transitions ("ODT" and "OOT") are thermoreversible. The data obtained as a function of temperature during the cooling process were superposed on those during the heating process. The influence

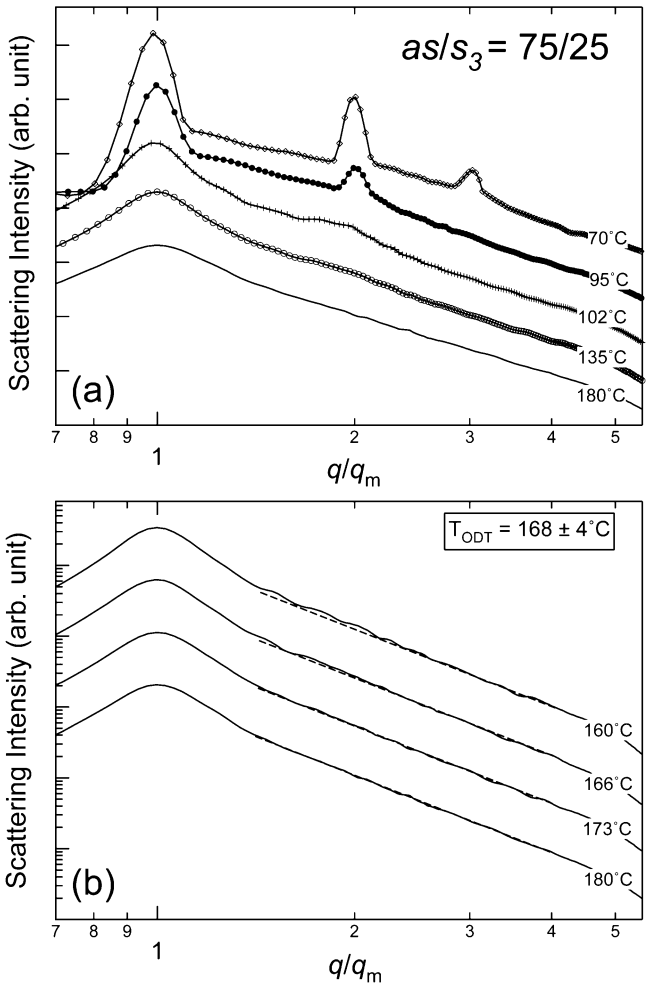

Figure 4. SAXS profiles of the *as*/s_3 = 75/25 mixture measured at different temperatures: (a) from 70 to 180 °C, where the mixture undergoes "OOT" (between 95 and 102 °C) as well as "ODT" (between 135 and 180 °C). (b) in the vicinity of the "ODT" where the broken lines underneath the measured profiles (solid lines) are visual guides for the presence of the second-order broad peak or shoulder on the profiles. In both (a) and (b), the scattering curves are vertically shifted from each other by a factor of 5. The horizontal axis is not q itself but normalized by q_m.

of the temperature on D is dramatically different from that observed on the *as*/s_3 = 45/55 mixture (cf. Figures 5c and 3c). As for the *as*/s_3 = 75/25 mixture, D decreases with increasing temperature in the whole temperature range studied. This decrease of D is particularly pronounced when the mixture has a lamellar morphology, but the trend itself is consistent with that reported for the neat block copolymer. It seems that the thickness of lamella and temperature can be related by a power law: $D \sim T^{-1.53}$. This result is significantly different from that obtained for the pure block copolymers or its solution[21]: $D \sim T^{-0.33}$. This large difference between pure block copolymers and this mixture (*as*/s_3 = 75/25) seems to be attributed to a particular organization of the diblock chains *as* and s_3 in the lamellar microdomains (the double brush layer structure, schematically depicted later in Figure 9a), which is thought to be a manifestation of a cosurfactant effect in a parameter space of temperature. However, a definitive interpretation is not yet established.

IV. Discussion

IV.1. Real-Space Observation of "OOT". In this section we shall further discuss the "OOT" presented by *as*/s_3 = 45/55

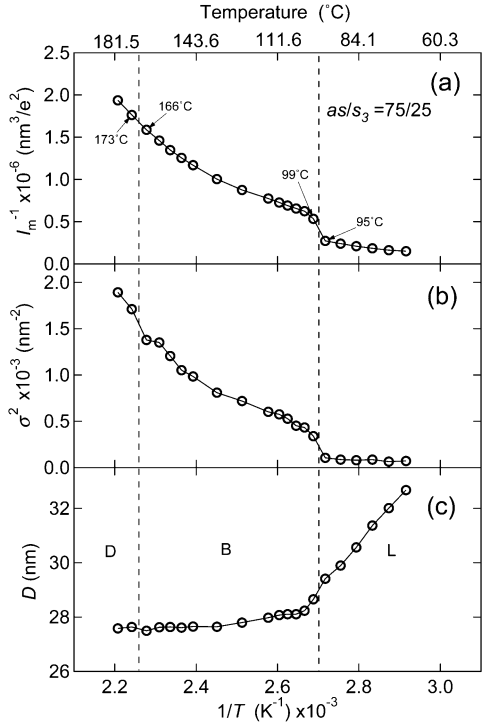

Figure 5. Plots for the $as/s_3 = 75/25$ mixture: influence of the temperature on inverse of the first-order peak intensity, I_m^{-1} (a), on square of the half-width at half-maximum of the first-order peak, σ_q^2 (b), and on the characteristic length of the microdomains or concentration fluctuations, D (c).

and 75/25 (w/w) mixtures. In fact, the morphology of the ordered phase that appears above the lamellar phase and below the disordered phase cannot be identified definitely from the SAXS profiles. On the other hand, the TEM method does not allow us to conduct an in-situ observation of this microdomain structure. Nevertheless, in the case of our system it is possible to circumvent this difficulty. Since the $T_{g,PS}$ is higher than the ambient temperature, the microdomain structure of the sample can be frozen below $T_{g,PS}$. Therefore, it is possible to freeze the structure stable at high temperatures below T_g without changing the structure and to observe it under TEM. Moreover, the scattering intensity profile of sample measured in situ at any temperatures was compared with that measured after quenching. The comparison between these two profiles allows us to evaluate the efficiency or feasibility of the quench.

Figure 6 shows the measured SAXS profiles of the $as/s_3 = 75/25$ mixture: one is at 110 °C before quench, and the other is at ambient temperature after the quench as described above. These two profiles were not corrected for TDS. We can confirm that these two profiles are almost identical, and therefore the quench was effective. The two scattering profiles at q/q_m around 1 are really the same so that the global structure are truly conserved through the quenching process, except for a slight change of q_m due to thermal expansion. The scattering profile measured in situ at 110 °C before quench is slightly higher than that at ambient temperature after quench at $q/q_m > 1.5$. The intensity difference at large q/q_m (≥ 4) is due to the difference in TDS. Since the higher the temperature is, the larger is the TDS intensity; the observed difference is reasonable. The intensity difference at q/q_m around 2−3 may be due to the difference in volume fraction of the minority microphase of PS, ϕ_{PS}; ϕ_{PS} is larger in situ at 110 °C before quench than at ambient temperature after quench due to a thermal expansion of PS domain, which may increase the intensity at 110 °C relative to

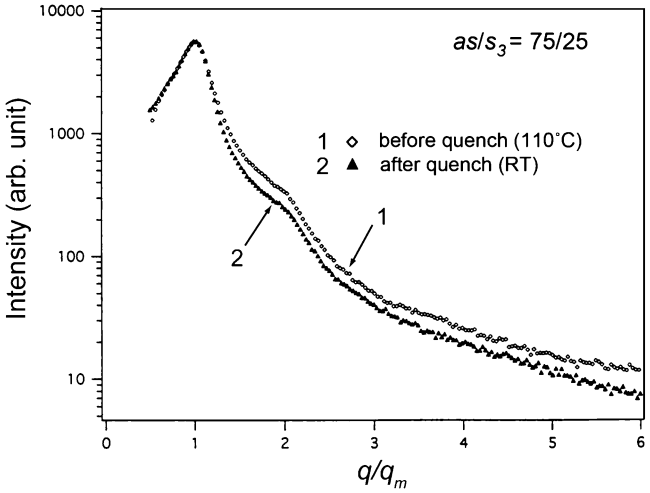

Figure 6. SAXS profiles of the $as/s_3 = 75/25$ mixture; the profile 1 indicated by open diamonds (◇) denotes the sample measured in situ at 110 °C, and the profile 2 indicated by filled triangles (▲) denotes that after the quench from 110 °C and measured at ambient temperature.

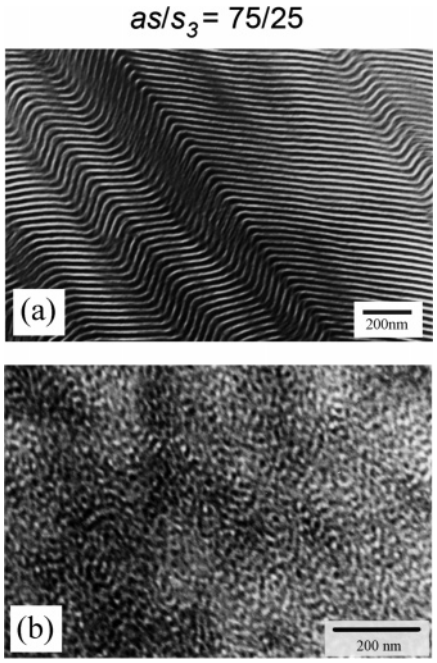

Figure 7. TEM micrographs of the $as/s_3 = 75/25$ mixture: lamellar morphology is equilibrium at ambient temperature (a), and the distorted bicontinuous morphology is obtained from the specimen annealed at 110 °C and then quenched into ice water (b).

that at ambient temperature. However, a quantitative verification of this deserves future works.

Figure 7b shows a TEM micrograph of this quench sample which represents successfully the structure at 110 °C, while Figure 7a shows a TEM micrograph of lamellar morphology observed on the same mixture at ambient temperature as equilibrium morphology. The mixture $as/s_3 = 45/55$ exhibited a similar morphology, though not shown here. The morphology of Figure 7b is quite similar to another as/s_3 mixture which forms bicontinuous morphology at ambient temperature (for example, the $as/s_3 = 82/18$ mixture, whose TEM micrograph is presented in the previous paper of this series of work[1]). Therefore, the combination of the real-space study by TEM and the reciprocal-space study by SAXS allows us to conclude that the intermediate phase of $as/s_3 = 45/55$ and 75/25 mixtures between lamellar and "disorder" is a "distorted bicontinuous

phase". However, this bicontinuous structure lacks such long-range order as observed for the lamellar structure, and its symmetry is unidentified after all, neither gyroid type[22] nor OBDD type.[23]

IV.2. Change of Segregation Power across "OOT" As Observed by Invariant *Q*. In this section we propose a method to study the state of segregation from the invariant as a function of temperature. This method is based on a classical technique of the small-angle X-ray scattering[15,24−26] and has an advantage coming from the fact that the invariant is independent of the morphology of the sample. If a material has the spatial variation of electron density, $\rho(r)$, or the amplitude of the electron density fluctuation from the average electron density $\langle\rho\rangle$, $\eta(r)$, $\rho(r) = \langle\rho\rangle + \eta(r)$, the mean square of $\eta(r)$, $\langle\eta^2\rangle$, is related to the invariant Q, the total scattering intensity from the system

$$\langle\eta^2\rangle \sim Q = 4\pi\int_0^\infty q^2 I(q)\,\mathrm{d}q \tag{2}$$

where $I(q)$ is the scattering intensity. Note that a change of domain structure such as from the lamellae to the distorted bicontinuous structure does not modify Q unless the structural changes alter $\langle\eta^2\rangle$. In the case of a system composed of two phases A and B with a sharp interface, whose electron densities are ρ_A and ρ_B, respectively, the expression of $\langle\eta^2\rangle$ is given by

$$\langle\eta^2\rangle = \phi(1-\phi)(\rho_A - \rho_B)^2 \tag{3}$$

where ϕ is the volume fraction of one of the two phases. Substituting this expression of $\langle\eta^2\rangle$ in eq 2, we obtain

$$Q = 4\pi\int_0^\infty q^2 I(q)\,\mathrm{d}q \sim \phi(1-\phi)(\rho_A - \rho_B)^2 \tag{4}$$

In the temperature range where the constituent two phases of the material are strongly segregated, and the electron density of each phase and ϕ are constant, Q is constant according to eq 4. Contrarily, when the two phases become weakly segregated, a part of A blocks exists in the B microdomains and vice versa, and the electron density difference, $|\rho_A - \rho_B|$, between the two coexisting microdomains decrease with temperature, Q decreases with temperature. Thus, the temperature dependence of the segregation power can be monitored by temperature dependence of Q.

It should be noted here that according to the theory of small-angle X-ray scattering, the invariant is calculated as integral of $I(q)q^2$ from $q = 0$ to infinity, while experimentally $I(q)$ is measured and integrated only from $q = 0.05$ nm^{-1} to $q = 1.6$ nm^{-1}. An error caused by the truncation of the integral is not so important in this work because we are not interested in the absolute value of Q but rather in relative change of Q with temperature. Note further that, as already described in section II.2, $I(q)$ is corrected for TDS, and therefore its contribution to Q was eliminated.

The results of the estimation on the mixtures of $as/s_3 = 45/55$ and $as/s_3 = 75/25$ are represented respectively in parts a and b of Figure 8. The value of Q for $as/s_3 = 45/55$ is always larger than that for $as/s_3 = 75/25$ (part a). This can be rationally explained as follows. According to eq 4, Q becomes large as ϕ approaches 0.5, or the compositions PS and PI phases become symmetric. Compared with $as/s_3 = 75/25$, $as/s_3 = 45/55$ which contains a larger amount of the symmetric block copolymer (s_3) is more symmetric and hence shows a higher Q value. The two specimens $as/s_3 = 75/25$ and 45/55 show a similar trend in Figure 8a: At low temperatures Q is nearly independent of $1/T$, while at high temperatures Q monotonically increases with $1/T$,

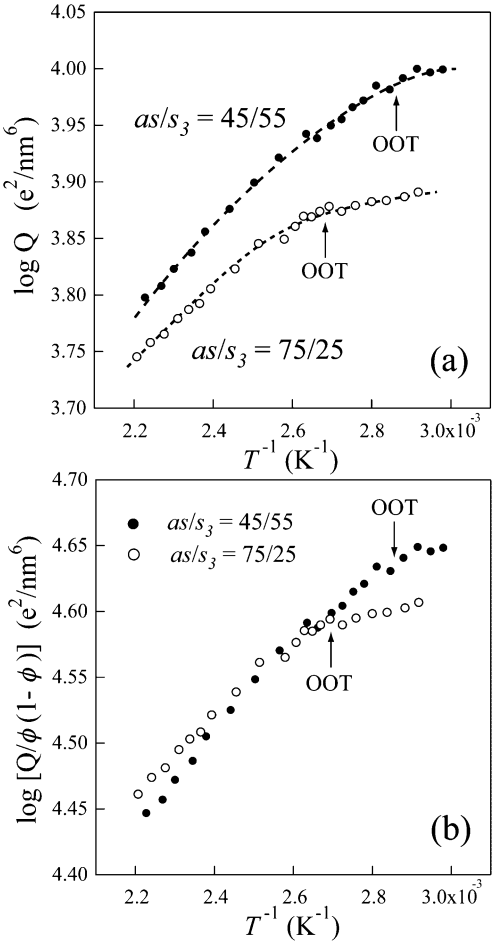

Figure 8. Change of the segregation power evaluated through the invariant Q as a function of the inverse of the temperature: semilogarithmic plot of log Q vs T^{-1} for $as/s_3 = 45/55$ and 75/25 mixtures (a) and that of normalized invariant, i.e., $\log[Q/\{\phi(1-\phi)\}]$ vs T^{-1} for $as/s_3 = 45/55$ and 75/25 mixtures (b).

and the temperatures where the crossover is observed in log Q vs $1/T$ coincide with "OOT". Thus, in the lamellar phase Q hardly depends on $1/T$, but in the distorted bicontinuous phase Q decreases with decreasing $1/T$. It should be also noted that there is no discontinuity in Q at the "OOT", suggesting a continuous change of Q or $(\rho_A - \rho_B)^2\phi(1-\phi)$ at "OOT".

Figure 8b shows $\log[Q/\{\phi(1-\phi)\}]$ vs $1/T$. If ϕ does not change significantly with T, $\log[Q/\{\phi(1-\phi)\}] = \text{constant} + \log(\rho_A - \rho_B)^2$ so that this quantity is closely related to an intermixing of unlike segments within each domain and hence to a segregation power between the two blocks as a function of temperature. In the low-temperature range where the lamella phase exists, the segregation power for the 45/55 mixture is higher than that for 75/25, while in the high-temperature range where the distorted bicontinuous phase exists, $(\rho_A - \rho_B)^2$ for both mixtures decreases almost linearly and similarly with decreasing $1/T$. It is very important to note that **$(\rho_A - \rho_B)^2$ does not change at "OOT"**, as will be detailed below.

The change of microdomain structure at "OOT" kept the invariant almost constant. This indicates that spatial reorganization of the microdomains occurs without involving significant modification of the phase volume fraction ϕ and electron density difference of the two phases $(\rho_A - \rho_B)^2$ and the fraction of the diffuse interface region between the coexisting microdomains. This point seems to give **a serious problem** for the assertion of the distorted bicontinuous phase as a part of the disordered phase in the context of the current theory. We can conclude

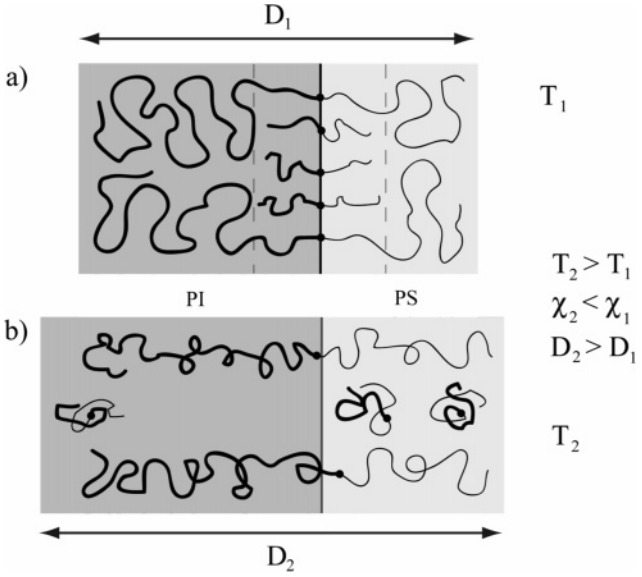

Figure 9. Schematic representation of the effect of the temperature on the delocalization of the short diblock s_3 in the lamella microdomains.

that this "OOT" is not induced by delocalization of junction points of short diblocks s_3 from the interface and solubilization of them into microdomains formed by the large molecular weights *as* block copolymers. It is rather related to a fine modification of the balance between the enthalpic effect (incompatibility between monomers A and B) and entropic (chain stretching), like ordinary "OOT" commonly observed on pure block copolymers.

The segregation power between PS and PI blocks seems to be almost independent of temperature in the low-temperature lamellar phase but tends to sharply decrease with increasing temperature in the high-temperature phase of distorted bicontinuous phase. The fact that the $as/s_3 = 45/55$ has a steeper slope of Q as a function of reciprocal temperature than $as/s_3 = 75/25$ may suggest that the delocalization of short diblock s_3 from the interface with increasing temperature is more outstanding in the $as/s_3 = 45/55$ mixture than in the $as/s_3 = 75/25$ mixture. This issue is further discussed in detail in the next section and will be clarified by analyzing the intriguing difference in the behavior of D vs $1/T$ for the two mixtures.

IV.3. Cosurfactant Effects as a Function of Temperature. As mentioned above, $as/s_3 = 45/55$ falls into in the weak segregation limit at high temperatures, and the short diblock s_3 is expected to be delocalized from the interface. This delocalization of s_3 can rationally explain an anomalous temperature dependence of D, as shown in Figure 3c. Parts a and b of Figure 9 give schematic illustrations of the chain organization model for $as/s_3 = 45/55$ at low and high temperatures, respectively. At low temperatures (Figure 9a), the junctions of short diblocks s_3 are well localized at the interface, and the microdomains are regarded to be divided into two layers: one is composed of mixed brushes of *as* and s_3, and the other is composed of only *as* brush. The boundary between the two layers is depicted by a broken line parallel to the interface. This model is the so-called BZL model,[27] and short s_3 copolymers, which acts as cosurfactant with long *as* copolymers, may effectively decrease the domain size, D, and decrease the interface curvature to stabilize the lamellar phase. On the other hand, at high temperatures (Figure 9b), short diblocks tend to depart from interface and swell the microdomains. As a consequence, the domain size is dominated by long diblocks *as* and become bigger than that of low temperatures. Note that this speculation is corroborated by combined SAXS and SANS (small-angle neutron scattering) observation for a similar block copolymer mixture system; namely, the mixture consists of a long asymmetric PS−PI copolymer (PS-rich) and a short symmetric dPS−PI copolymer, where dPS denotes deuterated polystyrene having a large scattering length for the neutron beam.[28]

On the other hand, the mixture $as/s_3 = 75/25$ shows a normal temperature dependence of D similar to the neat block in a sense that D decreases with increasing T, which is primarily due to a decrease of segregation power with T. However, the following two points are worth being noted. (i) $D \sim T^{-1.53}$ for the lamellar phase of $as/s_3 = 75/25$ rather than $D \sim T^{-0.33}$ found for neat block copolymers having the lamellar phase; (ii) In the distorted bicontinuous phase D for the mixture decreases only slightly with $1/T$ than D for the lamellar phase. The former phenomenon (i) is expected to be related to the cosurfactant effects described earlier. The latter phenomenon (ii) is anticipated to be a consequence of a balance of the following two opposing effects: (a) a decrease of D with increasing T due to the decrease of segregation power in the case when junctions of s_3 are kept in the thickened interfacial region; (b) an increase of D with increasing T due to the depart of junctions of s_3 from the interface. Localization of s_3 at the domain interface may be more stable for $as/s_3 = 75/25$ than for $as/s_3 = 45/55$ because of the smaller concentration of s_3 for the former mixture. Thus, the temperature dependence of the delocalization of s_3 for the former mixture may be less than that for the latter mixture. In any case these phenomena are intricately coupled with the cosurfactant effects as a function of temperature.

The existence of the distorted bicontinuous phase in the mixtures of as/s_3 is in part due to the cosurfactant effect, especially for $as/s_3 = 75/25$, and in part due to the blending effect, especially for $as/s_3 = 45/55$. This is because the junctions of s_3 tend to be kept at the interface to a greater degree for the 75/25 mixture than for the 45/55 mixture or because they tend to be delocalized from the interface to a greater degree for the 45/55 mixture than for the 75/25 mixture. The cosurfactant effect seems to enlarge the bicontinuous phase.

IV.4. Time-Resolved Studies of "OOT" Process. Here we are interested in the way how the bicontinuous → lamella transition occurs, namely, to try to understand how the microdomains of PS and PI which are continuous in three-dimensional space transform into lamella which is continuous only in two dimension. From this point of view a kinetic study of the bicontinuous → lamella transition by SAXS and TEM was conducted for the $as/s_3 = 75/25$ mixture.

A specimen of the $as/s_3 = 75/25$ mixture which was preannealed in the disordered state is slowly cooled to the lowest temperature in the stable region of the bicontinuous morphology. Then it is annealed for 1 h at this temperature, and the scattering profile was measured. Without removing the specimen from the SAXS apparatus its temperature was decreased by 5 °C to settle the specimen at a temperature where the lamellar morphology is stable. The temperature of the specimen reached equilibrium within 5 min. After attaining temperature equilibration the scattering profile of the specimen was measured several times at intervals of 10 min. This method allows to follow the time evolution of the scattering profile and therefore the morphology of the specimen. The scattering profiles measured in such a way, before, during, and after "OOT", are shown in Figure 10. The transition is observed through a change in the first-order peak and also by the transformation of the shoulder at $q/q_m \cong 1.9$ to the peak at $q/q_m = 2$. It seems that the intensity profile changes rapidly with time in early stage and then evolves

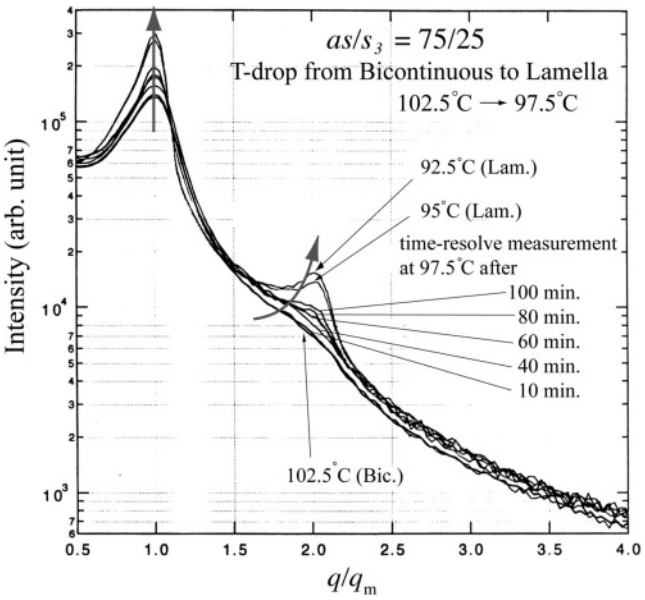

Figure 10. SAXS profiles of the as/s_3 = 75/25 mixture, indicating the process of "OOT" from bicontinuous to lamellar phase with decreasing temperature: the profiles before (at 102.5 °C), during (at 97.5 °C and at different intervals from 10 to 100 min), and after the transition at 95 and 92.5 °C are shown.

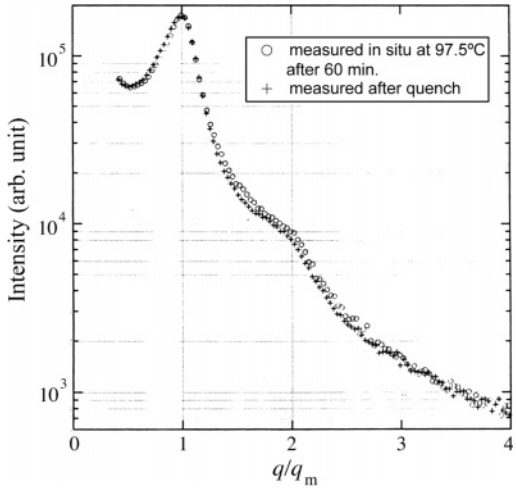

Figure 11. SAXS profiles of the as/s_3 = 75/25 mixture, measured in situ at 60 min after onset of the transition from bicontinuous to lamella (○) at 97.5 °C and measured after the quench (+). The thermal diffuse scattering was subtracted from the net observed scattering profiles for both cases.

more slowly until to the end of measurement at 100 min. Each measured profiles during the transition were able to be decomposed into a linear combination of the profile from the lamellar morphology at 97.5 °C and that from the bicontinuous morphology at 102.5 °C. This seems to indicate that during the phase transition the lamellar morphology and the bicontinuous morphology coexist in the specimen. Gradually the fraction of bicontinuous phase decreases and that of the lamellar phase increases.

We tried to confirm the above result by TEM. A specimen of the as/s_3 = 75/25 mixture was subjected to the same thermal protocol as the preceding one employed for SAXS measurement, but the process of the bicontinuous → lamella transition was interrupted by the quenching as described earlier. In Figure 11, the SAXS profile of the quenched specimen, which was measured at ambient temperature, is compared with the profile measured in situ at 60 min after onset of the transition at 97.5 °C. We can confirm that the quench was effective; the two curves are essentially identical. It should be worthy of comparing Figures 6 and 11: both are showing a good coincidence of the profiles before and after the quench; however, the coincidence in Figure 11 is much better than that in Figure 6. This difference can be rationalized by the following two factors. First, the profiles shown in Figure 6 are not subjected for the TDS corrections, but those in Figure 11 were corrected for TDS. This accounts for the difference in the coincidence of the two data sets in Figures 6 and 11 at large values of $q/q_m \geq 4$. The effect of TDS on the scattering profiles at large q values was discussed earlier in section IV.1. Second, the dynamics of microdomains or concentration fluctuations abruptly slows down at the temperatures close to $T_{g,PS}$. Therefore, the structure at 97.5 °C could be well trapped by quench due to a proximity of the temperature to $T_{g,PS}$ (Figure 11), whereas the structure at 110 °C could be changeable during the quenching process (Figure 6). A possible change involved by the quenching process was discussed earlier in section IV.1.

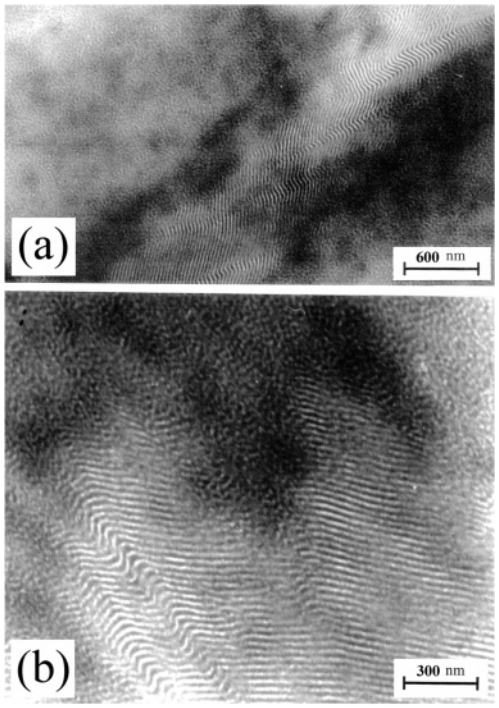

Figure 12. TEM micrographs of the as/s_3 = 75/25 mixture: the specimen is quenched during the process of "OOT" from bicontinuous to lamella. The coexistence of two morphologies can be observed. At a low magnification, an anisotropic lamellar grain, which is elongated in the direction parallel to lamellar normal, is in the matrix of bicontinuous morphology (a), and at high magnification; the interfacial area between the coexisting two phases is focused (b).

The observation by TEM of this quenched specimen is shown in Figure 12, which reveals that there are two types of morphologies (the bicontinuous morphology and a regular stack of lamellae). These results corroborate those obtained by SAXS: during the "OOT" the two phases coexist, and the transformation from the bicontinuous structure to the lamellar structure developed via the nucleation growth process. The observation of TEM images over a large area of this specimen indicated that the nucleuses of the lamellar phases are anisotropic. They seem always more extended in the direction parallel to lamella normal than the other directions. This anisotropy is probably induced by the anisotropic interfacial free energy on the interface between the nuclei of lamellae and the matrix of the bicontinuous phase (referred to as LB interface hereafter).

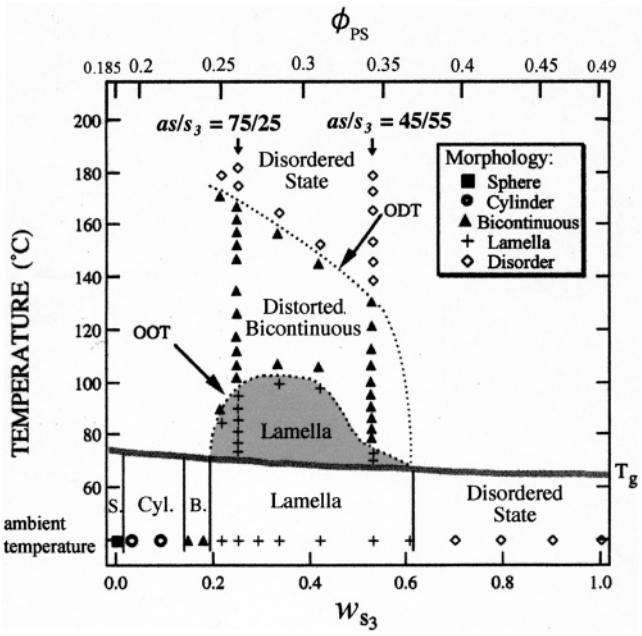

Figure 13. Partial phase diagram of as/s_3 mixtures in the parameter space of temperature and the weight fraction of s_3. The mixtures, which have lamellar morphology at ambient temperature and undergo "OOT" (lamella/bicontinuous) and "ODT", especially $as/s_3 = 45/55$ and 75/25, are featured. A complete phase diagram of the as/s_3 mixture system will be presented in a forthcoming paper.[30]

We can consider two kinds of interface and its interfacial free energy as to LB interface: one is the transverse interface where the LB interface is perpendicular to the lamellar interfaces (or parallel to the lamellar normal) with interfacial free energy denoted as $\sigma_\perp$ hereafter. The other is the longitudinal interface where the LB interface is parallel to the lamellar interface (or perpendicular to the lamellar normal) with interfacial free energy denoted as $\sigma_\parallel$. Since $\sigma_\perp < \sigma_\parallel$ is anticipated from the conformational entropy loss in packing of the block copolymer chains at the LB interface, the nucleus is expected to have large extension along the lamellar normal than along the lamellar interface. It is worthy of noting that in the case of order−disorder transition (ODT) of low-molecular-weight SI copolymer a similar anisotropic lamellar nucleus is observed in the disordered matrix.[2,3] Moreover, near ODT, $\sigma_\perp < \sigma_\parallel$ is corroborated by the theoretical work of Hohenberg and Swift.[29] There is striking similarity between our study and that of Sakamoto and Hashimoto,[3] except that in our study the matrix is the distorted bicontinuous phase instead of the disordered phase.

V. Conclusion

The influence of the temperature on the morphology of a series of mixtures comprised of a long and asymmetric diblock copolymer *as* and a short and symmetric diblock copolymer s_3 was investigated in detail. Especially the mixtures which possess lamellar morphology at ambient temperature and therefore whose "cosurfactant effect" is conspicuous are featured in this study. As summarized in the partial phase diagram of Figure 13, these mixtures showed a similar phase behavior along the temperature axis, namely the lamellar structure first transforms into the distorted bicontinuous structure and finally becomes the disordered state with increasing temperature. We summarize once again the cosurfactant effects in conjunction with this phase diagram. First, the low-temperature lamellar phase is expanded down to the total volume fraction of PS blocks ϕ_{PS} equal to 0.245, while the corresponding ϕ_{PS} for neat block copolymer is extended only down to 0.32. The extended composition range of ϕ_{PS} for the lamellar phase decreases with increasing temperature so that the extended lamellar phase due to the cosurfactant effect exists in the dome-shaped region which is shown by a shaded region in the parameter space of temperature and w_{s3} or ϕ_{PS}.

It may be worthy of commenting possible reasons for dome-shaped "OOT" phase boundary between lamellar and distorted bicontinuous phases. The increase of T_{OOT} with w_{s3} from $w_{s3} = 0.2$ to 0.3 is explained by an effect of increasing overall composition ϕ_{PS}; namely, the lamellar phase is more stabilized than the bicontinuous phase when the total volume fraction of PS is increased to 0.5. At the same time, the increase of the fraction of s_3 decreases the segregation power of the system and therefore decreases the stability of lamellar phase with T. In other words, the bicontinuous phase is expanded with respect to T compared to that of lamellar phase. This effect causes the decrease of T_{OOT} with w_{s3}. These two opposing effects can explain qualitatively the dome shape of T_{OOT} vs w_{s_3} in Figure 13. On the other hand the "ODT" phase boundary monotonically decreases with increasing w_{s3}, reflecting the fact that the long diblock copolymer *as* is much strongly segregated than the short diblock s_3.

Second, for a neat block copolymer a bicontinuous phase (double-gyroid phase) exists in a very narrow region in the parameter space of temperature and ϕ_{PS}, near the boundary between cylinder phase and lamellar phase. The cosurfactant effect seems to enlarge the parameter space where the bicontinuous phase appears, though the phase is considerably distorted in terms of long-range order. This is especially true for the mixture having a large fraction of *as*, e.g., the 75/25 mixture.

It should be mentioned in conclusion that although only the "OOT" between the lamellar structure and the distorted bicontinuous structure is highlighted in this study, the as/s_3 mixtures includes much richer phase behavior with a variety of morphologies, which should be addressed in a forthcoming companion paper.[30]

References and Notes

(1) Court, F.; Hashimoto, T. *Macromolecules* **2001**, *34*, 2536; **2002**, *35*, 2566.
(2) Hashimoto, T.; Koga, T.; Koga, T.; Sakamoto, N. In *The Physics of Complex Liquids*; Yonezawa, F., Tsuji, K., Kaji, K., Doi, M., Fujiwara, T., Eds.; World Scientific: Singapore, 1998; pp 291−308.
(3) Sakamoto, N.; Hashimoto, T. *Macromolecules* **1998**, *31*, 3815.
(4) Leibler, L. *Macromolecules* **1980** *13*, 1602.
(5) Hamley, I. W. *The Physics of Block Copolymers*; Oxford University Press: Oxford, 1998.
(6) Hasegawa, H.; Hashimoto, T. In *Comprehensive Polymer Science, Second Supplement*; Aggarwal, S. L., Russo, S., Vol. Eds.; Pergamon: Oxford, England, 1996; p 497.
(7) Lin, E. K.; Gast, A. P.; Shi, A.-C.; Noolandi, J.; Smith, S. D. *Macromolecules* **1996**, *29*, 5920.
(8) Shi, A.-C.; Noolandi, J. *Macromolecules* **1994**, *27*, 2936.
(9) Zhao, J.; Majumdar, B.; Schulz, M. F.; Bates, F. S.; Almdal, K.; Mortensen, K.; Hajdak, D. A.; Gruner, S. M. *Macromolecules* **1996**, *29*, 1204.
(10) Fujimura, M.; Hashimoto, T.; Kawai, H. *Mem. Fac. Eng., Kyoto Univ.* **1981**, *43*, 224.
(11) Hashimoto, T.; Suehiro, S.; Shibayama, M.; Saijo, K.; Kawai, H. *Polym. J.* **1981**, *13*, 501.
(12) Suehiro, S.; Saijo, K.; Ohta, Y.; Hashimoto, T. *Anal. Chim. Acta* **1986**, *189*, 41.
(13) Guinier, A.; Fournet, G. *Small-Angle Scattering of X-rays*; J. Wiley & Sons: New York, 1955.
(14) Brumberg, H., Ed.; *Small-Angle X-ray Scattering*; Gordon & Breach: New York, 1965.
(15) Balta-Calleja, F. J.; Vonk, C. G. *X-ray Scattering of Synthetic Polymers*; Elsevier: Amsterdam, 1989.
(16) Hendricks, R. W. *J. Appl. Crystallogr.* **1972**, *5*, 315.

(17) (a) Kato, K. *J. Polym. Sci., Polym. Lett. Ed.* **1966**, *4*, 35. (b) Ribbe, A. E.; Bodycomb, J.; Hashimoto, T. *Macromolecules* **1999**, *32*, 3154.
(18) Sakamoto, N.; Hashimoto, T. *Macromolecules* **1995**, *28*, 6825.
(19) Stühn, B.; Mutter, R.; Albrecht, T. *Europhys. Lett.* **1992**, *18*, 427.
(20) Wolff, T.; Burger, C.; Ruland, W. *Macromolecules* **1993**, *26*, 1707.
(21) Hashimoto, T.; Shibayama, M.; Kawai, H. *Macromolecules* **1983**, *16*, 1093.
(22) Hajduk, D. A.; Harper, P. E.; Gruner, S. M.; Honeker, C. C.; Kim, G.; Thomas, E. L.; Fetters, L. J. *Macromolecules* **1994**, *27*, 4063.
(23) Thomas, E. L.; Alward, D. B.; Kinning, D. J.; Martin, D. C.; Handlin, D. L.; Fetters, L. J. *Macromolecules* **1986**, *19*, 2197. Hasegawa, H.; Tanaka, H.; Yamasaki, K.; Hashimoto, T. *Macromolecules* **1987**, *20*, 1651.
(24) Alexander, L. E. *X-ray Diffraction Methods in Polymer Science*; Wiley: New York, 1969; Chapter 5.
(25) Ruland, W. *J. Appl. Crystallogr.* **1971**, *4*, 70.
(26) Roe, R. J.; Gieniewski, C. *Macromolecules* **1973**, *6*, 212.
(27) Birshtein, T. M.; Liatskaya, Y. V.; Zhulina, E. B. *Polymer* **1990**, *31*, 2185. Zhulina, E. B.; Birshtein, T. M. *Polymer* **1991**, *32*, 1299.
(28) Yamaguchi, D.; Bodycomb, J.; Koizumi, S.; Hashimoto, T. *Macromolecules* **1999**, *32*, 5884.
(29) Hohenberg, P. C.; Swift, J. B. *Phys. Rev. E* **1995**, *52*, 1828.
(30) Court, F.; Yamaguchi, D.; Hashimoto, T. Manuscript in preparation.

MA0525233